



1,8-Cineole promotes G0/G1 cell cycle arrest and oxidative stress-induced senescence in HepG2 cells and sensitizes cells to anti-senescence drugs

Boris Rodenak-Kladniew^{a,b,*}, Agustina Castro^a, Peter Stärkel^{c,d}, Marianela Galle^a, Rosana Crespo^{a,b,*}

^a Instituto de Investigaciones Bioquímicas de La Plata (INIBIOLP), CONICET-UNLP, CCT-La Plata, La Plata, Argentina

^b Cátedra de Biología, Facultad de Ciencias Médicas, Universidad Nacional de La Plata, La Plata, Argentina

^c Laboratory of Hepato-Gastroenterology, Institut de Recherche Expérimentale et Clinique, Université Catholique de Louvain, Brussels, Belgium

^d Department of Gastroenterology, Cliniques Universitaires Saint-Luc, Brussels, Belgium

ARTICLE INFO

Keywords:

1,8-Cineole
Hepatocellular carcinoma cells
Cell cycle arrest
Senescence
Oxidative stress
MAPKs
AMPK
Akt/mTOR

ABSTRACT

Aims: 1,8-Cineole is a plant-derived monoterpene and a major constituent of Eucalyptus essential oil. Previously, we demonstrated that 1,8-cineole inhibited hepatocellular carcinoma (HCC) HepG2 cell growth. However, the underlying mechanisms remain unknown. Here, we evaluated the mechanisms of action of 1,8-cineole and the potential benefits of its combination with anticancer compounds harboring “anti-senescence” properties in HepG2 cells.

Main methods: Cell viability was determined by the MTT assay. Cell cycle was assessed through flow cytometry (FC) and western blot (WB). Senescence was determined by the SA- β -galactosidase assay, and apoptosis by caspase-3 activity, WB, and TUNEL. MAPKs (ERK, JNK, and p38), AMPK, and Akt/mTOR were analyzed by WB. Reactive oxygen species (ROS) and mitochondrial membrane potential ($\Delta\Psi_m$) were evaluated by FC and fluorescence microscopy.

Key findings: 1,8-Cineole inhibited cell proliferation by promoting G0/G1 arrest. While 1,8-cineole was unable to trigger apoptosis, it induced cellular senescence. 1,8-Cineole promoted ROS production, $\Delta\Psi_m$ depolarization, AMPK, ERK, and p38 activation and mTOR inhibition. Antioxidants, like N-acetyl-L-cysteine and vitamins, prevented HepG2 cell growth inhibition and senescence induced by 1,8-cineole. Pre-incubation with 1,8-cineole sensitized HepG2 cells to the anti-senescence compounds, quercetin, simvastatin, U0126, and SB202190. Combinations of 1,8-cineole and each compound synergistically inhibited cell viability, and combined treatment with 1,8-cineole and simvastatin induced apoptosis.

Significance: 1,8-Cineole induces G0/G1 arrest and senescence in HepG2 cells through oxidative stress and MAPK, AMPK, and Akt/mTOR pathways, and sensitizes cells to anti-senescence drugs, suggesting that 1,8-cineole has potential as an antineoplastic and adjuvant compound in combination with anti-senescence drugs in HCC therapy.

1. Introduction

Liver cancer is the second most common cause of cancer death worldwide, with an incidence of about 800,000 new patients per year. Hepatocellular carcinoma (HCC) is the most frequent primary liver malignancy (75–90%) and is characterized as highly recurrent and treatment-resistant, with a mortality-to-incidence ratio of 0.95 [1,2]. HCC commonly does not respond to conventional chemotherapy. Safer and more effective chemopreventive and chemotherapeutic compounds are thus required to be able to develop novel and/or complementary therapies. Small molecular target agents, monoclonal antibodies and

multikinase inhibitors have emerged as possibilities for HCC treatment [1].

Nature is an excellent source of potential anticancer drugs. Approximately 50% of the drugs currently used in clinics are natural-based products. In particular, plants and herbs are an inexhaustible source of phytochemicals with potential antitumor activities, and many of these (alkaloids and taxanes) have widely been employed in cancer therapy for several years [5].

Terpenes are natural isoprenoids found in essential oils of plants and herbs with, for example, analgesic, anxiolytic, antimicrobial, and anti-tumor activities. Several studies showed that these compounds have

* Corresponding author at: Cátedra de Biología, Facultad de Ciencias Médicas, Universidad Nacional de La Plata, La Plata, Argentina

E-mail addresses: brodenak@med.unlp.edu.ar (B. Rodenak-Kladniew), ro_crespo@yahoo.com (R. Crespo).

<https://doi.org/10.1016/j.lfs.2020.117271>

Received 30 August 2019; Received in revised form 26 December 2019; Accepted 3 January 2020

Available online 08 January 2020

0024-3205/ © 2020 Elsevier Inc. All rights reserved.

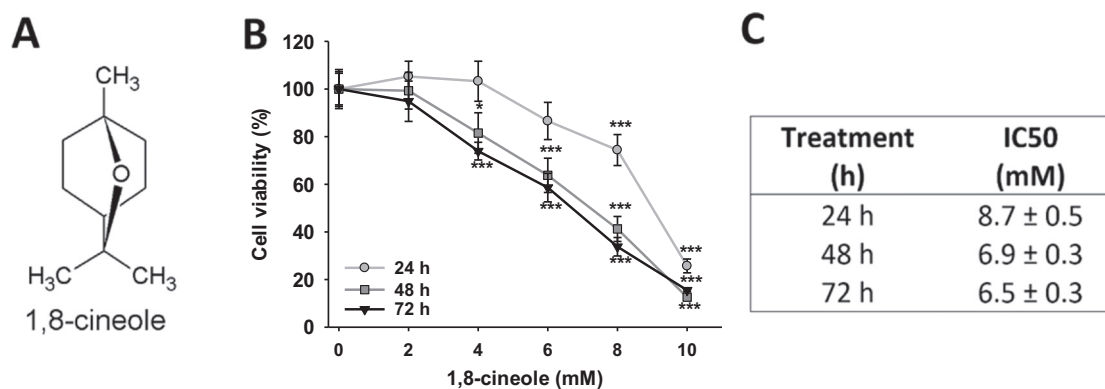


Fig. 1. Effects of 1,8-cineole on HepG2 cell viability. (A) Structural formula of 1,8-cineole. (B) HepG2 cells were incubated for 24, 48 and 72 h with increasing concentrations of 1,8-cineole (0–10 mM). Data are presented as the mean \pm SD. * $p < 0.05$; *** $p < 0.001$. (C) IC50 values obtained from non-linear regression curves.

chemopreventive and chemotherapeutic activities both in vitro and in vivo [6]. The main molecular targets include the Ras/Raf/MEK/ERK and Akt/mTOR pathways [6], commonly deregulated and implicated in HCC development and progression [7]. A wide variety of these plant-derived compounds also act as anticancer agents by promoting the generation of reactive oxygen species [8,9], which inhibit cancer progression [10]. ROS play a central role as signaling molecules by inducing stress-responsive mitogen-activated protein kinase (MAPK), AMPK, Akt and mTOR modulation and/or mitochondrial damage which results in cell cycle arrest, apoptosis, senescence and/or autophagy of cancer cells [11–14].

1,8-Cineole (Fig. 1A), also known as eucalyptol, is a cyclic-ether monoterpene present in essential oils of several plants including tea, rosemary, sage, bay, cinnamon and is the major constituent of eucalyptus essential oil [15]. Numerous biological and pharmacological applications have been reported for 1,8-cineole, including expectorant, penetration enhancer, anti-inflammatory, antibacterial, antifungal [16–18] and to a much lesser extent, as an anticancer compound [19–22]. We reported for the first time that 1,8-cineole inhibits the cell growth of hepatocellular carcinoma (HepG2) and lung adenocarcinoma (A549) cells [23]. However, the mechanisms of action involved remain poorly understood.

The aim of this study was to shed light on the mechanisms of action responsible for the antiproliferative effects of 1,8-cineole in HepG2 HCC cells and to evaluate in vitro its potential as a neoadjuvant or co-adjuvant molecule when combined with anticancer anti-senescence drugs.

2. Materials and methods

2.1. Reagents and antibodies

1,8-Cineole (> 99%), Propidium iodide (PI), 2,7-dichlorodihydrofluorescein diacetate (DCFH-DA), *N*-acetyl-L-cysteine (NAC), rhodamine-123 (Rh-123), quercetin (Qc), simvastatin (Sv), U0126 (U), and SB202190 (SB) were obtained from Sigma Chemical Co. (St Louis, MO, USA). Protease and phosphatase inhibitors were from Thermo Scientific (Rockford, USA). Other chemicals from local suppliers were of analytical grade. Antibodies for phospho-ERK (Thr202/Tyr204), phospho-JNK (Thr183/Tyr185), phospho-p38 (Thr180/Tyr182), p38, phospho-Akt (Ser473), phospho-AMPK (Thr172), phospho-70S6K (Thr389) were from Cell Signaling Technology (Danvers, MA, USA). Antibodies for p21, p27, p53, Cdk6, Cdk4, Cdk2, cyclin A, cyclin D1, cyclin E, PARP, caspase-3, caspase-9, and p70S6K were from Santa Cruz Biotechnology (Santa Cruz, CA, USA). Antibodies for ERK and Akt were from BD Biosciences (Erembodegem, Belgium). Anti- β -actin and anti-GAPDH antibodies were from Sigma (St Louis, MO).

2.2. Cell culture

HepG2 cells (ATCC® HB-8065™) were obtained from the American Type Culture Collection and maintained in Dulbecco's Minimal Essential Medium (DMEM) supplemented with 10% fetal bovine serum and 1% streptomycin and penicillin (Gibco, Invitrogen, Carlsbad, CA) in a humidified atmosphere at 37 °C and 5% CO₂. The medium was renewed every 48 h. For experiments, the cells were seeded at a density of 1–3 $\times 10^3$ cells/cm² and allowed to adhere 24 h before the beginning of treatments. The number of cultured cells was adjusted to a density such that the cells grew exponentially before initiating the experimental incubations.

2.3. Cell viability

The MTT assay (3-(4,5-dimethylthiazol-2-yl)-2,5-diphenyltetrazolium bromide) was used to evaluate cell viability. HepG2 (5 $\times 10^3$) cells were seeded in 96-well plates and cultured under standard conditions for 24 h. The cells were then treated with DMEM supplemented with ethanol 0.2% (vehicle) or 1,8-cineole (0–10.0 mM) for 24, 48 or 72 h. After washing with PBS, cells were incubated with MTT solution (0.5 mg/ml in PBS) for 3 h. The resulting formazan crystals were dissolved in 0.1 ml DMSO and the absorbance at 560 nm was measured with a Beckman Coulter DTX 880 microplate reader.

2.4. Cell cycle analysis

HepG2 cells (3 $\times 10^5$) were plated in 6-well plates and grown for 24 h. The cells were then incubated with ethanol 0.2% (control) or 1,8-cineole (4.0 and 8.0 mM) for 24 or 48 h, harvested by trypsinization, centrifuged at 500 $\times g$ for 5 min, resuspended in PBS and fixed in 70% ethanol – 20 °C overnight. Then, cells were washed twice with PBS and treated with ribonuclease A (500 U/ml; Biodynamics, Buenos Aires, Argentina) for 30 min at 37 °C. Nuclei were stained with PI (0.025 mg/ml) in the dark for 30 min and cells were analyzed by flow cytometry (BD FACSAriaII, BD Biosciences). DNA content was quantified by FlowJo version X 10.0.7r2 (Tree Star, Ashland, OR, USA).

2.5. Senescence-associated β -galactosidase (SA- β -gal) activity assay

The SA- β -gal activity assay was performed as previously reported [24]. Briefly, HepG2 cells (1.5 $\times 10^4$) plated in 24-well plates were incubated with ethanol 0.2% v/v or 1,8-cineole (4.0 and 8.0 mM) for 24, 48 or 72 h. The cells were then incubated in fresh medium for an additional 72 h. The cells were then fixed in 3.7% paraformaldehyde in PBS, washed with PBS and incubated in SA- β -gal staining solution [1 mg/ml 5-bromo-4-chloro-3-indolyl-b-D-galactopyranoside (X-gal),

40 mM citric acid sodium phosphate, pH 6.0, 5 mM potassium ferrocyanide, 5 mM potassium ferricyanide, 150 mM NaCl, and 2 mM $MgCl_2$] at 37 °C for 12–14 h in the dark. HepG2 cells were washed twice with PBS and then examined under a Leica DMIL light microscope (Leica, Wetzlar, Germany).

2.6. Detection of apoptosis by TUNEL assay

HepG2 cells (3×10^5) plated on sterile coverslips (24×24 mm) in 6-well plates were incubated for 24 or 48 h with ethanol 0.2%, 1,8-cineole 4 mM or 8 mM. Apoptosis was determined by terminal deoxynucleotidyl transferase-mediated dUTP nick end labeling (TUNEL) assay (In-Situ Cell Death Detection Kit, TMR Red, Roche, Mannheim, Germany) according to the manufacturer's instructions. The slides were mounted with ProLong® Gold Antifade Reagent with DAPI (4',6-diamidino-2-phenylindole dihydrochloride) for nuclear staining (Life Technologies, Carlsbad, CA, USA) and examined under an Olympus BX51 Fluorescence Microscope (Tokyo, Japan) equipped with an Olympus DP70 digital camera. Images were analyzed using ImagePro Plus v. 5.1 software (Media Cybernetics, Silver Spring, MD, USA).

2.7. Measurement of caspase-3 activity

Caspase-3 activity was determined with the colorimetric Caspase-3 Assay Kit (Sigma, St. Louis, MO, USA) following the manufacturer's protocol.

2.8. Intracellular reactive oxygen species (ROS) measurement

Intracellular ROS generation was determined using the oxidant-sensitive fluorescent probe DCFH-DA (Sigma Aldrich), as previously described [25]. Briefly, HepG2 cells seeded in 24-well plates (5×10^4) were treated for 3 h with ethanol 0.2%, 1,8-cineole (4.0 and 8.0 mM), hydrogen peroxide 0.5 mM (positive control), or pretreated with NAC 5 mM 2 h prior to 1,8-cineole exposure. Then the cells were washed with PBS and incubated with 10 μ M DCFH-DA in the dark for 30 min at 37 °C.

Fluorescence intensity was detected under an Olympus LX71 Inverted Fluorescence Microscope (Tokyo, Japan) at an excitation wavelength of 488 nm and an emission wavelength of 525 nm. In parallel, after DCFH-DA staining, cells were washed, harvested in 1 ml PBS and DCF fluorescence was detected by flow cytometry (FACSCanto II, Becton Dickinson, Erembodegem, Belgium).

2.9. Evaluation of mitochondrial membrane potential ($\Delta\Psi_m$)

The loss of mitochondrial membrane potential ($\Delta\Psi_m$) was monitored with the fluorescent probe Rh-123, a cationic dye which preferentially accumulates in mitochondria in a $\Delta\Psi_m$ -dependent manner. HepG2 cells seeded in 24-well plates (5×10^4) were treated with different concentrations of 1,8-cineole (4.0 and 8.0 mM) and rotenone 5 μ M (positive control) for 3 h. Cells were washed twice with PBS and stained with 5 μ M Rh-123 in free-serum DMEM for 30 min at 37 °C in the dark, again washed three times with PBS and analyzed under an Olympus LX71 Inverted Fluorescence Microscope (Tokyo, Japan) at an excitation wavelength of 488 nm and an emission wavelength of 525 nm. Fluorescence intensity was analyzed by Image J 1.51k software.

2.10. Western blot analysis

HepG2 cells (2×10^6) seeded in 100 mm Petri dishes were allowed to adhere for 24 h and then exposed to 1,8-cineole 4.0 and 8.0 mM for 24 or 48 h. Cells were washed twice in PBS and lysed in RIPA lysis buffer supplemented with protease and phosphatase inhibitors. Total protein was quantified by BCA protein assay (Pierce, Rockford, IL,

USA). Protein samples (50 μ g) were resolved on a 10–12% SDS-PAGE and transferred to polyvinylidene difluoride membranes (Amersham GE, Munich, Germany). After blocking for 1 h at room temperature in 5% BSA in TBST buffer (150 mM NaCl, 10 mM Tris-HCl–pH 7.4, 0.05% Tween-20), membranes were incubated with primary antibodies (4 °C, overnight) and secondary antibodies (room temperature, 2 h). Protein bands were detected with the Western Lightning Chemiluminescence Reagent Plus (Perkin Elmer, Boston, MA, USA) detection system and quantified by densitometry analysis using the Molecular Imager Gel Doc XR System 170–8170 device and software (Bio-Rad, Nazareth, Belgium). Each protein band was normalized to GAPDH and phosphokinases were normalized to their total kinase (ERK, JNK, p38, Akt and p70S6K) or β -actin (AMPK).

2.11. Effect of N-acetyl cysteine and vitamins C and E on 1,8-cineole-induced HepG2 cell growth inhibition

HepG2 cells (5×10^3) seeded in 96-well plates were pre-incubated or not with NAC (5 mM) and the combination of vitamins C and E (50 μ M each), washed in PBS and then treated with 1,8-cineole (0–10 mM) or hydrogen peroxide 0.5 mM (positive control) for 24 and 48 h. Cell viability was evaluated by the MTT assay.

2.12. Evaluation of effects of combined treatments between 1,8-cineole and various anti-senescence compounds on cell viability

To evaluate the potential benefits of 1,8-cineole as a sensitizer or adjuvant compound in combined or in tandem therapies, HepG2 cells were pre-treated with 1,8-cineole before incubation with various anticancer anti-senescence compounds (in tandem) or co-treated with 1,8-cineole and each compound (combined). Qc, Sv, U (Ras/MEK/ERK inhibitor), and SB (p38 MAPK inhibitor) were selected, given that they have been reported to inhibit senescence-related pathways and/or preferentially promote senescent cell death [12,26–30]. HepG2 cells (5×10^3) seeded in 96-well plates were pre-treated with ethanol 0.2%, 1,8-cineole 4 mM (48 h) or 8 mM (24 h), before incubation with Qc 75 μ M, Sv 10 μ M, U 10 μ M or SB 10 μ M for another 24 h. In parallel, cells were co-treated with 1,8-cineole and the mentioned compounds at different concentrations for 24 or 48 h. Cell viability was determined by the MTT assay.

2.13. Statistics

Results are expressed as relative change compared with controls and presented as means \pm SD. Statistical significance was determined using the Student *t*-test. Significance was set at $p < 0.05$ (GraphPad InStat program). The IC50 values (concentration that inhibits cell viability by 50%) were calculated by nonlinear-regression curves (SigmaPlot software; Systat Software, Inc., Point Richmond, CA, USA).

3. Results

3.1. 1,8-Cineole decreased HepG2 cell growth in a dose- and time-dependent manner

To determine the antiproliferative concentrations of 1,8-cineole, HepG2 cells were treated with increasing concentrations of 1,8-cineole (0–10 mM) for up to 72 h, followed by the MTT assay. 1,8-Cineole significantly inhibited cell growth from 8 mM and 4 mM onward after 24 and 48 h, respectively. A dose-dependent effect was observed for all different time-course experiments while time-dependent differences were mainly observed between 24 and 48 h treatments (Fig. 1B). IC50 values obtained from dose-response curves are shown in Fig. 1C.

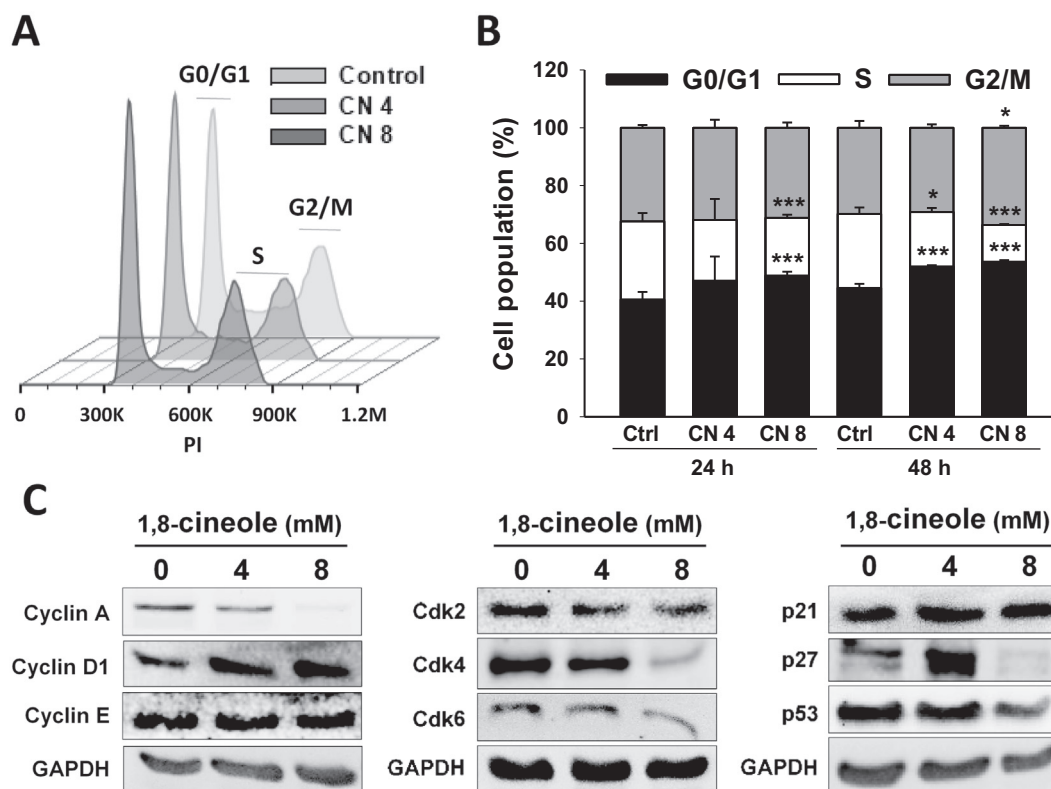


Fig. 2. 1,8-Cineole induces cell cycle arrest in HepG2 cells. (A–B) HepG2 cell cycle distribution after 24 h and 48 h treatments with 1,8-cineole (CN). (A) Representative histograms showing control and treated cell populations in G0/G1, S and G2/M phases. (B) Cell cycle distribution in HepG2 cells treated with CN 4 and 8 mM for 24 h and 48 h. Data are expressed as mean \pm SD (n = 4). *p < 0.05; ***p < 0.001. (C) Western blot analysis of cell cycle regulatory proteins cyclin A, cyclin D1, cyclin E, Cdk2, Cdk4, Cdk6, p21, p27, and p53. GAPDH was employed as a loading control to normalize protein expression.

3.2. 1,8-Cineole induced G0/G1 cell cycle arrest but not apoptosis in HepG2 cells

A cell cycle analysis was performed to explore the mechanisms by which 1,8-cineole inhibited HepG2 cell growth (Fig. 2). The G0/G1 cell population increased from 40.5% in control cells to 46.9 ($p = 0.10$) and 48.8% ($p < 0.05$) in cells exposed for 24 h to 1,8-cineole 4 and 8 mM, respectively. This effect was further amplified with the extension of treatment to 48 h (44.5% in control cells to 51.9 and 53.6% for 1,8-cineole 4 and 8 mM, respectively; $p < 0.05$). G0/G1 arrest was accompanied by a statistically significant decrease in S-phase cells after 24 h of treatment with 1,8-cineole 8 mM, peaking at 48 h (25.7% in controls vs. 12.6% in 1,8-cineole 8 mM) (Fig. 2B). To investigate the molecular events that caused G0/G1 arrest, the expression of cell cycle regulatory proteins involved in G1 progression and G1/S transition was evaluated by western blot (Fig. 2C). After 1,8-cineole 8 mM exposure, expression of Cdk2, Cdk4, Cdk6, and cyclin A strongly decreased ($p < 0.05$). Moreover, increased levels of p27 ($p < 0.01$) but not of p21, two well-known cyclin-dependent kinase inhibitors, were detected in cells treated with 1,8-cineole 4 mM. Cyclin D1 levels notably increased at both 1,8-cineole 4 and 8 mM ($p < 0.01$, Fig. 2D). Finally, no significant changes were observed for cyclin E and p53.

To determine whether cell apoptosis was involved as an anti-proliferative mechanism, we first analyzed caspase-3 activity, an effector caspase activated either by intrinsic or extrinsic pathways. Fig. 3A shows that no caspase-3 activation was observed in HepG2 cells after 24 or 48 h incubation with 1,8-cineole 8 mM. To further confirm that 1,8-cineole was incapable of inducing apoptosis, caspase-9 (initiator caspase from the intrinsic pathway), caspase-3, and PARP (substrate of effector caspases) were evaluated by western blot. No cleaved (activated) caspase-3 (Fig. 3B) or caspase-9 (Fig. 3C) was observed. Moreover, protein levels of procaspase-9 and PARP did not

change (Fig. 3C). Finally, DNA fragmentation, a hallmark of late apoptosis, was assessed by TUNEL assay. As expected, no TUNEL-positive cells were observed after exposure of HepG2 cells to 1,8-cineole 4 or 8 mM during 48 h (Fig. 3D).

3.3. 1,8-Cineole induced HepG2 cell senescence

Cellular senescence is an irreversible cell cycle arrest that occurs in response to stress signals and it seems to play a key role in impairing the proliferation of cancer cells resistant to apoptosis [29]. We analyzed the ability of 1,8-cineole to induce cellular senescence in HepG2 cells through the SA- β -galactosidase staining assay (Fig. 4A), calculating the percentage of SA- β -galactosidase positive cells. As shown in Fig. 4B, the number of HepG2 senescent cells substantially increased from 2.7, 2.1, and 4.0% in control cells to 5.2, 9.4, and 13.6% (1,8-cineole 4 mM), and 7.3, 15.4, and 22.8% (1,8-cineole 8 mM), after 24, 48, and 72 h treatments, respectively. Additionally, changes were observed in the morphology characteristics of senescent HepG2 cells, which adopted an enlarged and flattened morphology and increased nuclear size (Supplementary Fig. 1). Altogether, these and earlier results suggest that 1,8-cineole induced G0/G1 cell cycle arrest followed by cellular senescence in cultured HepG2 cells.

3.4. 1,8-Cineole induced oxidative stress and depolarization of mitochondrial membrane potential ($\Delta\Psi_m$)

Next, we evaluated whether oxidative stress was part of the mechanism involved in 1,8-cineole-induced cell growth inhibition, as we observed for other monoterpenes in previous studies [25]. HepG2 cells were exposed to 1,8-cineole in the absence or presence of the antioxidant NAC, and ROS generation was evaluated (Fig. 5A–B). As shown in Fig. 5A and quantified in Fig. 5B, 1,8-cineole 4 mM did not induce

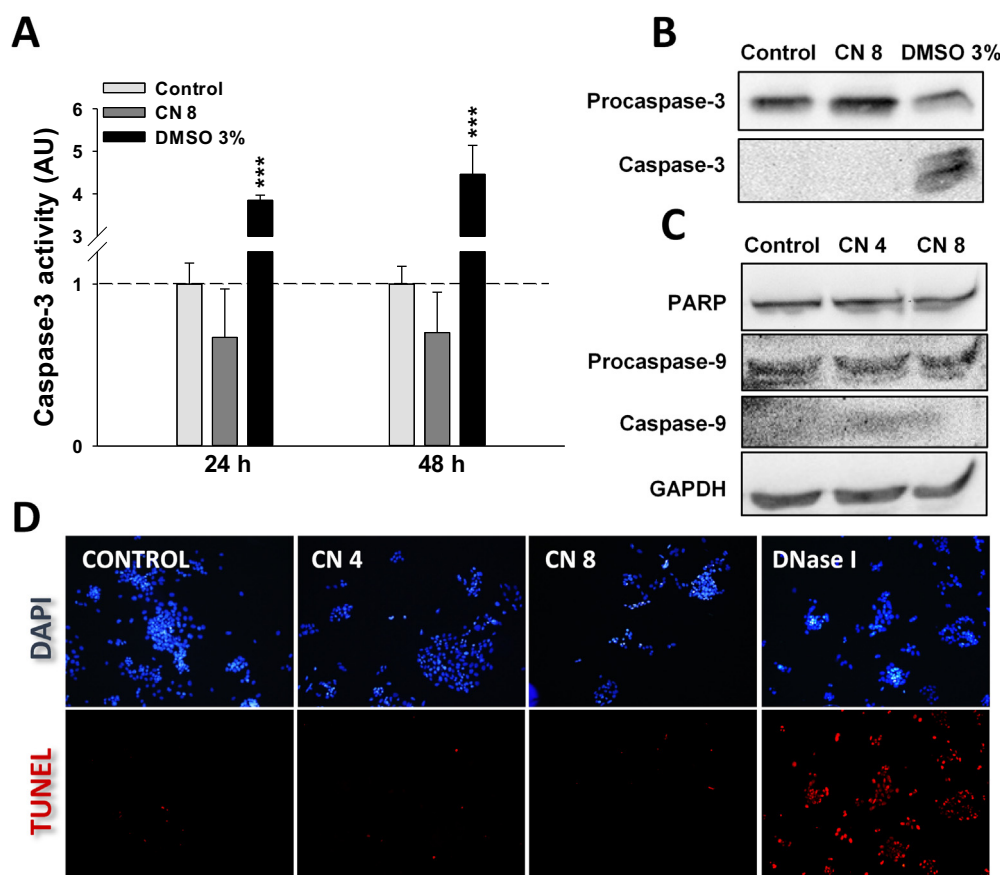


Fig. 3. Effect of 1,8-cineole on HepG2 cell apoptosis. Cells were incubated with 1,8-cineole (CN) for different durations (0, 24 and/or 48 h) and various apoptotic markers were evaluated. (A) Caspase-3 activity was determined with a commercial kit. DMSO 3% was employed as a positive control (AU = arbitrary units). Data are presented as the mean \pm SD; *** $p < 0.001$. (B–C) Representative western blot of caspase-3 (B), PARP and caspase-9 (C) after 48 h treatments. GAPDH was used as a loading control. (D) TUNEL assay was performed after 48-h treatments employing a commercial kit. Cells were treated with ethanol 0.2% (Control), CN 4 mM (CN 4), CN 8 mM (CN 8) or DNase I (30 min, positive control). Cells were examined under an Olympus BX51 fluorescence microscope (10 \times). Left panel, nuclei stained with DAPI; right panel, dUTP-rhodamine stained TUNEL positive cells. About 10–15 fields (100–200 cells/field) from three independent experiments were evaluated.

significant changes in ROS levels with respect to control cells. However, 1,8-cineole 8 mM moderately but significantly enhanced ROS production after 3-h treatments ($p < 0.001$), and pre-incubation with NAC 5 mM prevented 1,8-cineole-induced ROS, resulting in levels comparable to those of control cells.

Mitochondria is a major source of ROS, and excessive ROS levels evoke mitochondrial dysfunction. Both processes are known to be involved in cellular senescence [29,31]. Therefore, we evaluated Rh-123 incorporation in HepG2 cells after 3-h treatments with 1,8-cineole 4 and 8 mM (Fig. 5C) and found that 1,8-cineole 8 mM induced a 20.5% $\Delta\psi_m$ loss compared to control cells (Fig. 5D, $p < 0.001$).

3.5. Effect of antioxidants on 1,8-cineole induced cell growth inhibition and senescence

To evaluate the involvement of oxidative stress in HepG2 cell growth inhibition mediated by 1,8-cineole, cells were incubated with 1,8-cineole in the presence or absence of NAC (5 mM), or of a combination of vitamins C and E (50 μ M each one), for 24 and 48 h. In the presence of NAC, cell viability was restored from 74.3 to 94.3 after being exposed to 1,8-cineole 8 mM for 24 h ($p < 0.01$, Fig. 6A). NAC was even more effective in preventing 1,8-cineole-induced growth inhibition if treatment was prolonged for 48 h (Fig. 6B). Similar results were observed in the presence of vitamins C + E, which significantly diminished cell viability loss after exposure to 1,8-cineole ≥ 8 mM and 1,8-cineole ≥ 6 mM for 24 and 48 h, respectively (Fig. 6C–D).

To investigate whether 1,8-cineole-induced oxidative stress is responsible for the HepG2 cell senescence phenotype, we performed the SA- β -gal assay in HepG2 cells exposed to 1,8-cineole 4 and 8 mM for up to 72 h, pre-incubated or not with NAC 5 mM (Fig. 6E–F). In the presence of NAC, the number of SA- β -gal positive cells was reduced from 5.2 to 3.7% ($p = 0.3$), 9.4 to 3.8% ($p < 0.05$) and 13.6 to 5.1% ($p < 0.05$) after being incubated with 1,8-cineole 4 mM for 24, 48 and

72 h, respectively. When treated with 1,8-cineole 8 mM, HepG2 senescent cells were markedly reduced in the presence of NAC, from 7.3 to 3.5%, 15.4 to 3.7% and 22.8 to 6.8% after 24, 48, and 72 h treatments, respectively (Fig. 6F, $p < 0.05$ in all cases).

These results suggest that oxidative stress is strongly involved in HepG2 senescence induced by 1,8-cineole and that both ROS and senescence are responsible for the cell growth inhibition mediated by this monoterpene.

3.6. Modulation of MAPK, Akt/mTOR and AMPK signaling by 1,8-cineole

MAPK (ERK, JNK, and p38 kinases) signaling pathways are activated by phosphorylation in response to different stimuli including cellular stress, leading to cell survival or cell death [12,32]. Therefore, we first analyzed the time-(1–24 h, 1,8-cineole 8 mM) and dose-(24 h, 1,8-cineole 4 and 8 mM) effects of 1,8-cineole on ERK, JNK, and p38 phosphorylation. As shown in Fig. 7A, no changes in phospho-protein levels were detected for any of the three MAPKs after exposure to 1,8-cineole 4 mM. In contrast, 1,8-cineole 8 mM induced a significant 2-fold and 5.7-fold increase in ERK and p38 phosphorylation ($p < 0.05$), respectively, while phospho-JNK remained unaffected. When a time-dependent evaluation of MAPK phosphorylation was performed (Fig. 7B), we observed a sustained increase in phospho-ERK (p-ERK) from 1 to 24 h, while p-p38 expression peaked at 3 h and then remained high until 24 h.

Next, we assessed the effect of 1,8-cineole on surrogate markers of activation of the Akt/mTOR pathway, the main pro-survival anti-apoptotic signaling pathway related to chemoresistance of cancer cells. In comparison to control cells, 1,8-cineole 4 mM reduced Akt phosphorylation by 40% ($p < 0.05$), which was reversed in cells exposed to 1,8-cineole 8 mM (Fig. 7C).

Although 1,8-cineole 4 mM did not impact p70S6K phosphorylation, a 57% decrease in p70S6K phosphorylation was observed after

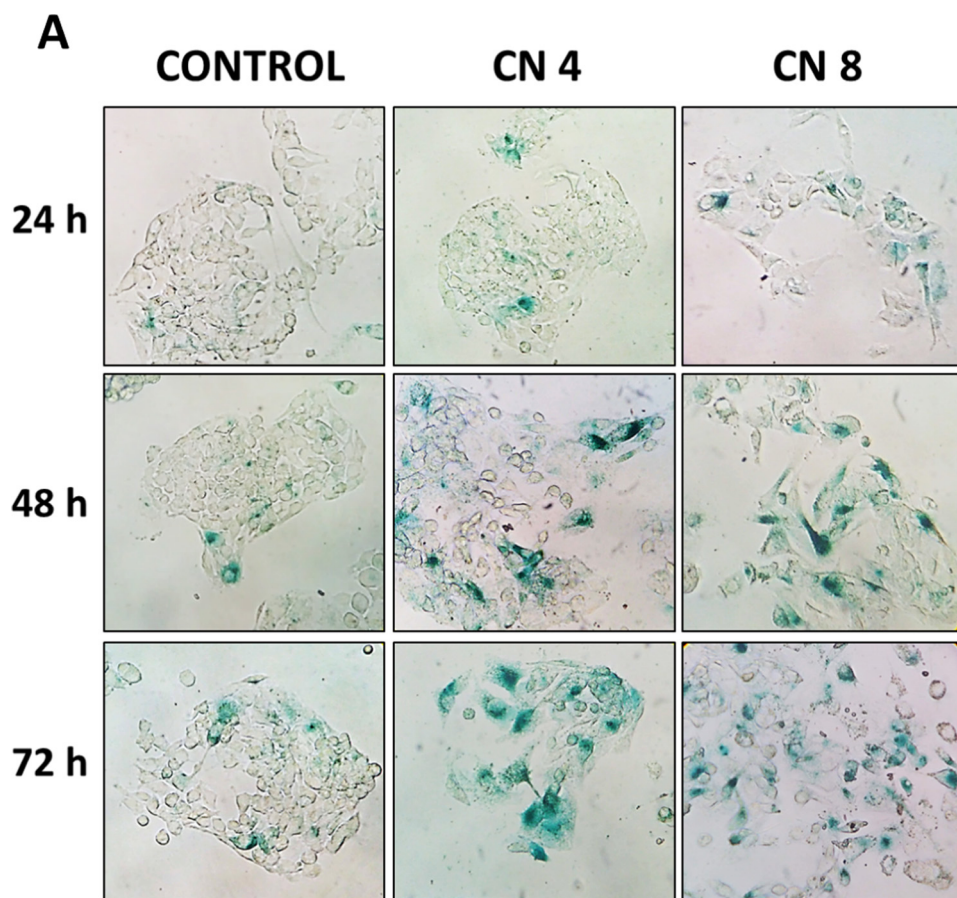
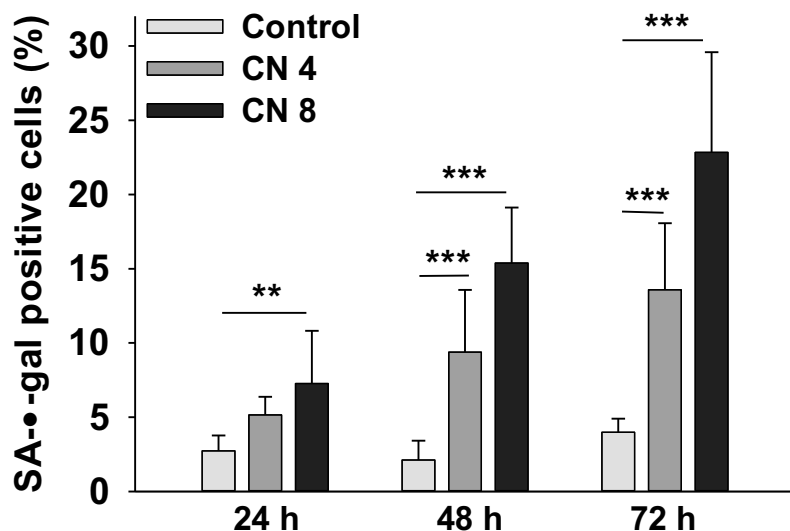


Fig. 4. Cellular senescence induced by 1,8-cineole (CN) in HepG2 cells. HepG2 cells were seeded in 24-well plates and treated with CN 4 mM (CN 4) or 8 mM (CN 8) for 24, 48 and 72 h. The cells were then cultured for another 72 h in fresh medium. SA-β-gal assay was performed as described in [Material and methods](#). SA-β-gal positive cells were stained blue. (A) Representative images obtained under a standard light microscope showing SA-β-gal positive HepG2 cells (blue cells). (B) Quantification of SA-β-gal positive cells. Data are presented as mean ± SD from three independent experiments. At least 800 cells for each treatment were evaluated. **p < 0.01; ***p < 0.001. (For interpretation of the references to color in this figure legend, the reader is referred to the web version of this article.)

B



1,8-cineole 8 mM treatment for 24 h ($p < 0.01$) (Fig. 7C). p-p70S6K levels were strongly diminished at 3 h ($p < 0.001$) and remained lower than controls for up to 24 h (Fig. 7D).

HepG2 cells exposed to 1,8-cineole 8 mM at different time points showed higher levels of p-Akt from 1 to 12 h, with a maximum at 3 h ($p < 0.001$, Fig. 7D).

Finally, we evaluated the phosphorylation of AMPK, a negative regulator of mTOR, which is activated in response to oxidative stress

and/or AMP/ATP ratio increase. 1,8-Cineole 4 mM did not affect AMPK phosphorylation after 24 h, but 1,8-cineole 8 mM induced a 50% reduction in p-AMPK ($p < 0.05$) compared to control cells (Fig. 7C). However, time-course experiments showed that 1,8-cineole 8 mM elicited a strong 5.9-fold increase in p-AMPK levels after 3 h incubation ($p < 0.001$), which remained high up to 12 h (Fig. 7D).

These results support the hypothesis that 1,8-cineole 8 mM induces cellular (oxidative) stress, which peaks at 1–3 h, promoting the

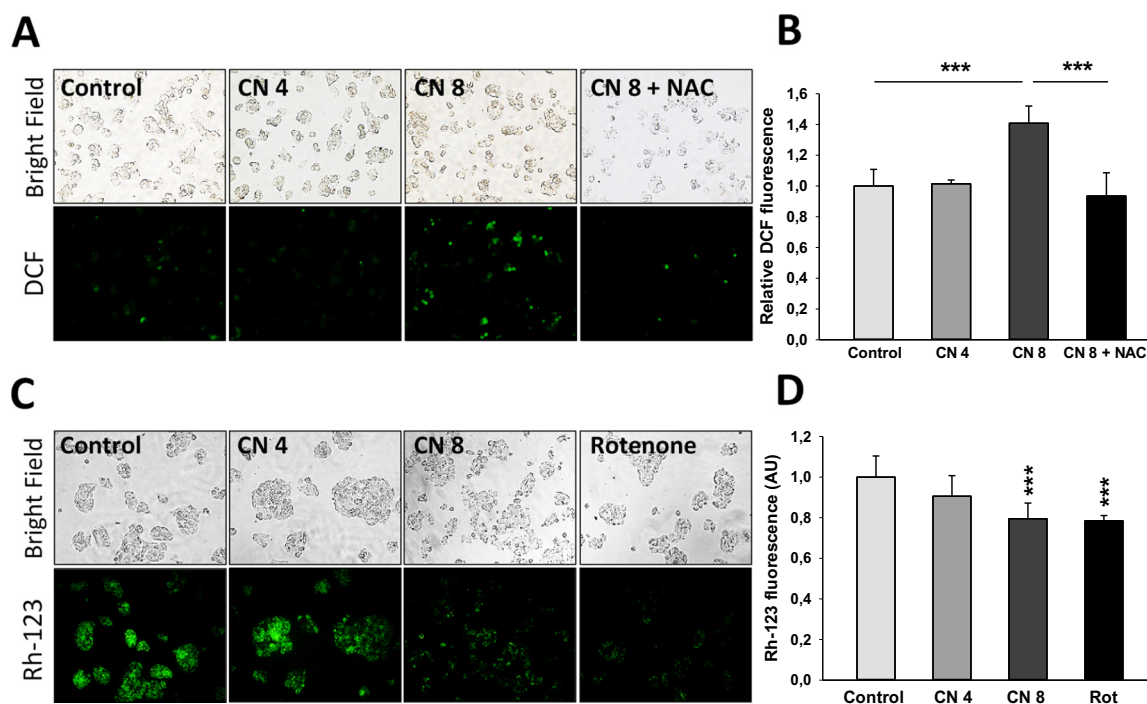


Fig. 5. Effects of 1,8-cineole (CN) on intracellular reactive oxygen species (ROS) and mitochondrial membrane potential ($\Delta\Psi_m$) in HepG2 cells. (A–B) HepG2 cells were treated with ethanol 0.2% (Control), CN 4 mM (CN 4), CN 8 mM (CN 8) or pre-incubated with NAC 5 mM 2 h prior to treatment with 1,8-cineole 8 mM (CN 8 + NAC) for 3 h. (A) Intracellular ROS production was analyzed under a fluorescence microscope (20 \times). (B) Quantitative analysis of DCF fluorescence analyzed by flow cytometry calculated relative to that of control (set at 1). (C–D) HepG2 cells were incubated with ethanol 0.2% (Control), CN 4 mM (CN 4), CN 8 mM (CN 8) or rotenone (positive control) for 3 h and then stained with Rh-123. (C) Cells were observed and photographed (40 \times) by light microscopy (upper panel) and under a fluorescence microscope (lower panel). (D) Quantitative analysis of Rh-123 green fluorescence in HepG2 cells. Data are presented as mean \pm SD. *** p < 0.001. (For interpretation of the references to color in this figure legend, the reader is referred to the web version of this article.)

activation of stress-responsive MAPKs, Akt, and AMPK kinases.

3.7. Combination of 1,8-cineole with anti-senescence compounds

HepG2 cells were pre-treated or not with 1,8-cineole 4 mM (48 h) and 1,8-cineole 8 mM (24 h) followed by incubation with Qc 75 μ M (Qc 75), Sv 10 μ M (Sv 10), U 10 μ M (U 10) or SB 10 μ M (SB 10) for 24 h (Fig. 8A). Pre-incubation with 1,8-cineole 4 mM (48 h) and 8 mM (24 h), as well as incubation of non-pre-treated cells with all compounds for 24 h, did not substantially affect HepG2 cell viability. However, when 1,8-cineole pre-treated cells were exposed to each of the four compounds for 24 h, cell growth inhibition was significantly enhanced compared with non-pre-treated cells (p < 0.001 in all cases), particularly in Sv treated cells (Fig. 8B–C).

To evaluate the potential of 1,8-cineole as an adjuvant in combined treatments, HepG2 cells were incubated for 24 or 48 h with 1,8-cineole, Qc, Sv, U, and SB, alone or in pairwise-combination of 1,8-cineole and each compound (Fig. 8D). Additive ($S = 1$) and synergistic effects ($S > 1$) were evaluated as described earlier [23]. As shown in Fig. 8E, HepG2 cells treated with 1,8-cineole 8 mM and each compound for 24 h presented synergistic growth inhibition when combined with Qc 75 ($S = 1.56$), Sv 10 ($S = 1.15$), U 10 ($S = 1.23$), and SB 10 ($S = 1.19$). Synergism was also found at 48 h when 1,8-cineole 4 mM was combined with Qc 50 ($S = 1.31$), Sv 5 ($S = 1.27$), U5 ($S = 1.25$) and SB 10 ($S = 1.27$) (Fig. 8F).

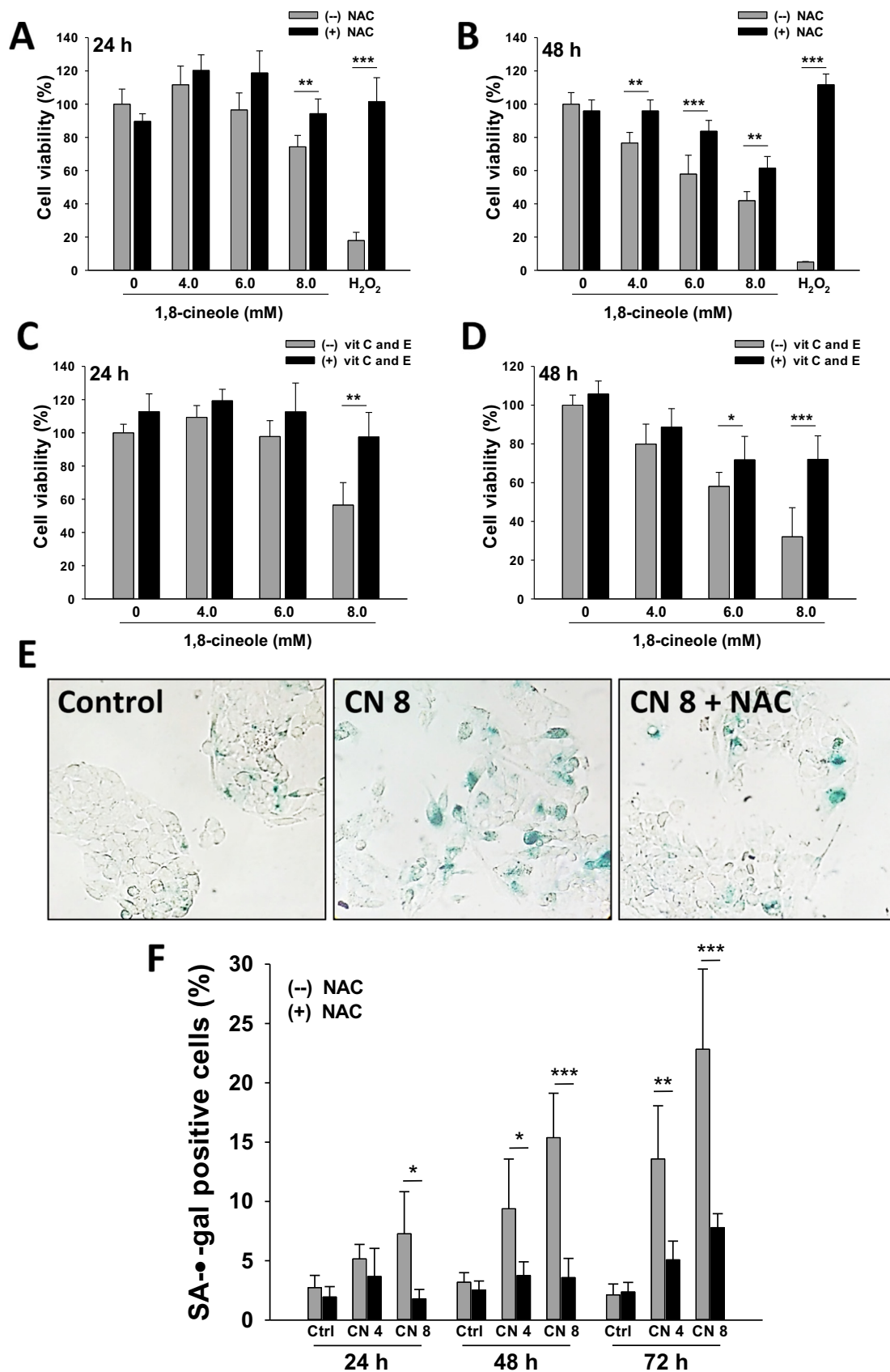
To get some insight into whether 1,8-cineole favors or sensitizes HepG2 cells to apoptosis in response to Sv, a TUNEL assay was performed for combined treatments of 1,8-cineole (4 mM) and Sv (5 μ M) for 48 h (Fig. 8G). As expected, no apoptosis induction was detected for any of the compounds tested alone. Nonetheless, a significant 5.3-fold increase in TUNEL-positive cells was found for the combined treatment compared to control cells (p < 0.01).

4. Discussion

Natural products are an exceptional source for novel drugs. Particularly, 1,8-cineole has been extensively investigated as an anti-microbial and anti-fungal molecule [17,18]. However, its potential as an anticancer compound remains barely explored. A small number of works report antiproliferative effects of 1,8-cineole in vitro against leukemia [20], oral [21], colon [19,33], cervical [34], skin [22] and ovarian [35] cancer cells, or in in vivo xenograft models [19]. Here, we reported for the first time on the antiproliferative mechanisms of action of 1,8-cineole against HCC cells. We observed that 1,8-cineole inhibited HepG2 cell viability in a dose- and time-dependent manner, at concentrations comparable to those reported by others [19,21,34,35]. Except for Dörsam et al., none of these reports accounted for the effects of 1,8-cineole on cell cycle progression [33].

As we observed an increase in G0/G1 phase cells exposed to 1,8-cineole, we analyzed the proteins that regulate the G1 progression and G1/S transition of the cell cycle. Activation of cyclin-D-dependent Cdk4 or Cdk6 is necessary for progression through G1, while cyclin A-Cdk2 and cyclin E-Cdk2 complexes regulate G1/S transition and S progression. 1,8-Cineole induced a strong reduction in Cdk2, Cdk4, Cdk6, and cyclin A expression. In addition, p21 and p27 are Cdk inhibitors which promote cell cycle arrest and senescence and mediate the anti-cancer effects of several compounds [36]. Here, p27 was upregulated at low concentrations of 1,8-cineole. No variations were observed in p21 levels, which is consistent with the fact that p53, its positive modulator, did not change significantly. These results suggest that the G0/G1 arrest induced by 1,8-cineole is due to Cdk2, Cdk4, Cdk6 and cyclin A inhibition, p27 induction, and is independent of the p53-p21 axis.

Apoptotic cell death is one of the chief mechanisms by which anti-neoplastic drugs eliminate cancer cells. Under our conditions, 1,8-cineole was unable to induce apoptosis, even in circumstances where cell



(caption on next page)

Fig. 6. Effect of antioxidants on HepG2 cell viability and senescence. (A–D) HepG2 cells were pre-incubated for 2 h with NAC 5 mM (A–B) or a mixture of vitamins C and E 50 μ M each (C–D), prior to the addition of 1,8-cineole for 24 and 48 h, respectively. Cell viability was determined by MTT assay. Data are presented as the mean \pm SD. * p < 0.05; ** p < 0.01; *** p < 0.001. (E–F) HepG2 cells were seeded in 24-well plates and treated with 1,8-cineole 4 mM (CN 4) or 8 mM (CN 8) for 24, 48 and 72 h in absence or presence of NAC. The cells were then cultured for another 72 h in fresh medium. SA- β -gal assay was performed as described in Section 2.5. (E) Representative images showing SA- β -gal positive HepG2 cells (stained blue) after exposed to 1,8-cineole 8 mM for 72 h in absence (CN 8) or presence (CN 8 + NAC) of NAC. (F) Quantification of SA- β -gal positive cells. Data are presented as mean \pm SD. A minimum of 800 cells for each treatment were evaluated. * p < 0.05; ** p < 0.01; *** p < 0.001. (For interpretation of the references to color in this figure legend, the reader is referred to the web version of this article.)

viability was strongly impaired. This may be related to the resistance of HCC to apoptosis, characterized by alterations in p53 expression/activation and enhanced activity of anti-apoptotic pathways like PI3K/Akt and Ras/ERK pathways [37]. Indeed, Lai et al. showed that high p53 expression induced apoptosis in HCC cells, but lower amounts elicited only cell cycle arrest [38].

Cellular senescence is a stress-induced response of proliferating cells, triggered by stimuli like telomere shortening, oxidative and DNA damage, and cellular stress. Senescence acts as a survival response, characterized by permanent cell cycle arrest in which cells exhibit specific phenotypical and molecular features. Some of the hallmarks of senescence include enlarged size, flattened shape, vacuolization, resistance to apoptosis, cyclin D1 accumulation, senescence-associated β -galactosidase (SA- β -gal) activity and the acquisition of the senescence-

associated secretory phenotype (SASP) [39–41]. The main pathways involved in senescence include p53/p21, p16/Rb activation, or Cdk4/Cdk6 inhibition, in the last instance, in a manner dependent or independent of p21 and p16 [29,40,42,43]. Previous reports showed the ability of some terpenes to elicit senescence in cancer cells, including HepG2 cells [44,45]. However, to our knowledge, this is the first report showing that 1,8-cineole induces senescence in cancer cells. Here, the SA- β -gal assay showed that 1,8-cineole induced HepG2 cell senescence in a dose- and time-dependent manner. Moreover, additional markers such as cyclin D1 accumulation, Cdk4/Cdk6 inhibition, and SA-changes in HepG2 cell morphology supported these findings.

Intracellular ROS are generated at physiological levels in normal cellular processes. Increased quantities of ROS promote tumorigenesis, while excessive oxidative stress can produce cancer cell death [46].

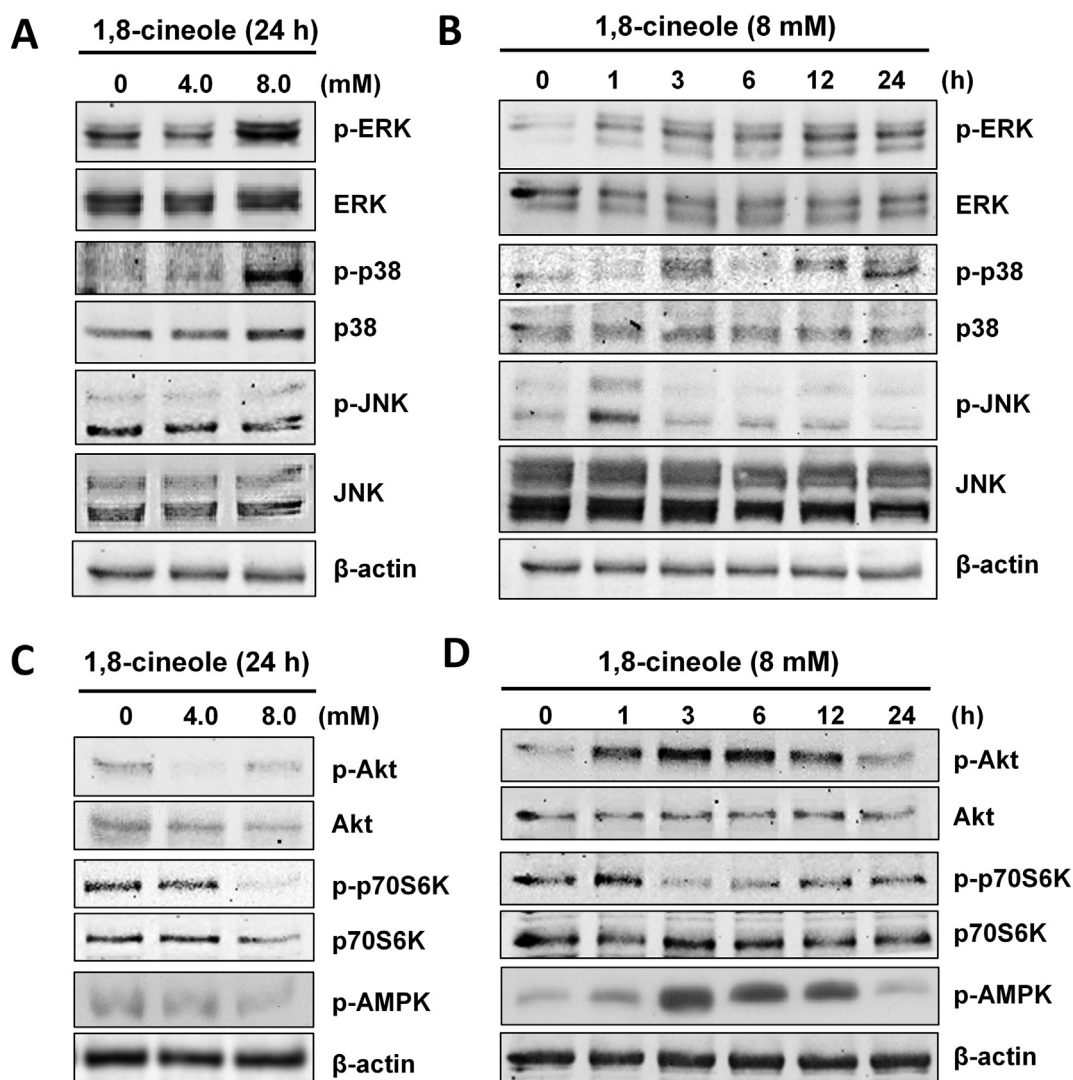


Fig. 7. Effect of 1,8-cineole on MAPK, Akt/mTOR and AMPK pathways. Western blot analysis showing the dose- (A, C) and time- (B, D) dependent effects of 1,8-cineole on MAPKs, Akt, AMPK and p70S6K in HepG2 cells. Immunoblot bands corresponding to phosphorylated and total protein of ERK, JNK, and p38 MAPK (A–B) and Akt, p70S6K and p-AMPK (C–D). β -Actin was employed as loading control.

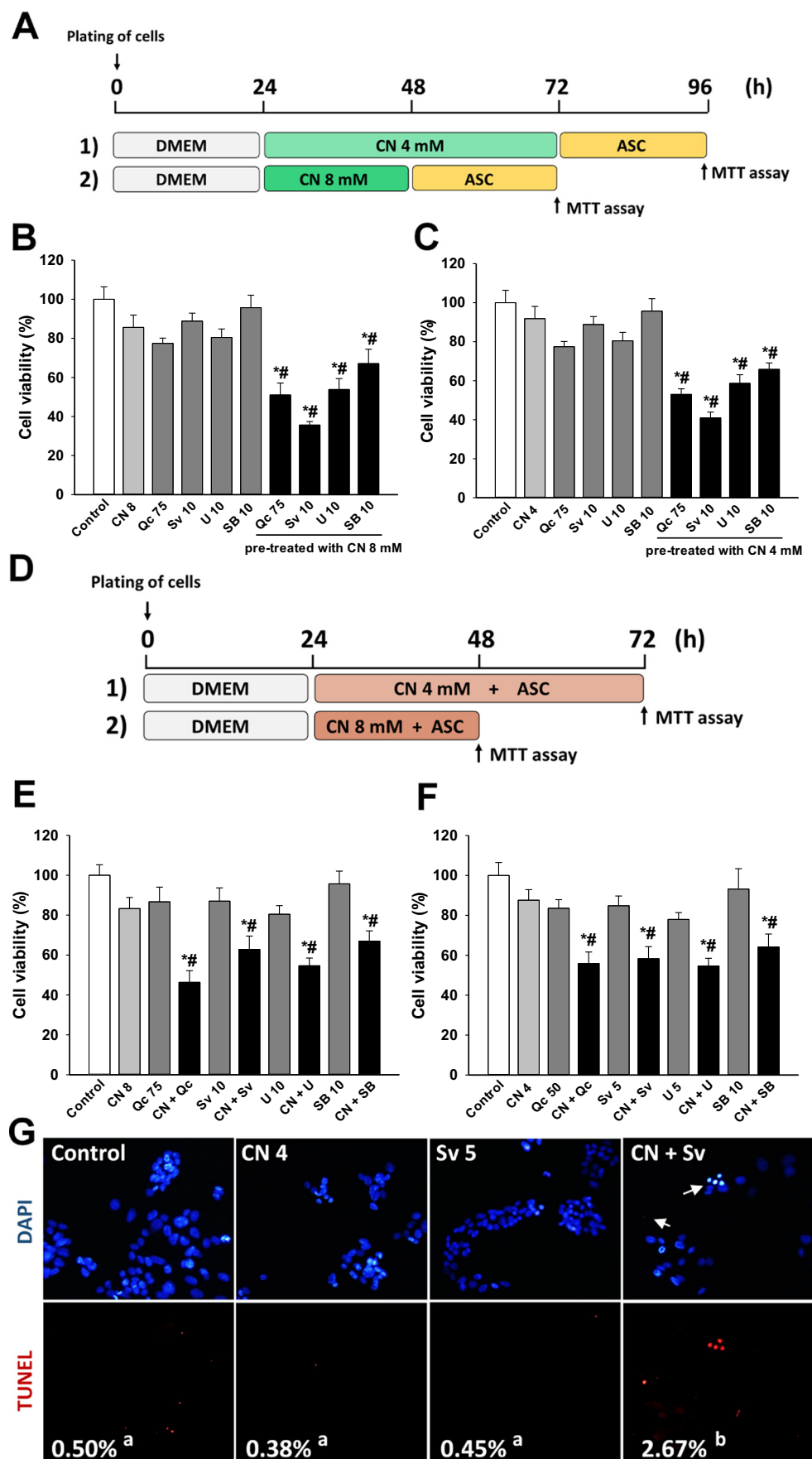


Fig. 8. Effect of 1,8-cineole (CN) as a sensitizer or adjuvant compound in tandem and combined treatments. (A) HepG2 cells were pre-incubated or not with CN 4 mM (CN 4) for 48 h (1) or CN 8 mM (CN 8) for 24 h (2). Then the cells were exposed to the anti-senescence compounds (ASC) Qc 75 μ M (Qc 75), Sv 10 μ M (Sv 10), U10 μ M (U 10) or SB 10 μ M (SB 10) for another 24 h. (B–C) Cell viability was determined by MTT assay. Data are presented as the mean \pm SD. * $p < 0.001$ vs. CN. # $p < 0.001$ vs. the same ASC alone. (D) HepG2 cells were treated with CN, Qc, Sv, U, and SB, alone or in pairwise combinations between CN and each compound for 24 (1) or 48 h (2). (E–F) Cell viability was determined by MTT assay. Data are presented as the mean \pm SD. * $p < 0.001$ vs. CN. # $p < 0.001$ vs. the same ASC alone. (G) HepG2 cells were treated with sub-effective concentrations of CN (CN 4), Sv (5 μ M, Sv 5) or with the combination of CN 4 + Sv 5 (CN + Sv). A TUNEL assay was performed after 48 h treatments, as described in Section 2. Cells were examined under an Olympus BX51 fluorescence microscope (10 \times) and analyzed as stated in Fig. 3D. Data are expressed as the mean \pm SD. Means without the same letter are different ($p < 0.01$).

Different studies in cancer cells suggest that low to moderately increased ROS levels trigger cytostatic autophagy, followed by cell cycle arrest and senescence, while higher amounts lead to cytotoxic cell death [41,42]. Indeed, Aravinthan et al. demonstrated that low concentrations of hydrogen peroxide elicited HepG2 cell senescence [47]. In this work, we found that 1,8-cineole is a weaker ROS inducer, as previously reported in colorectal cancer cells [33], and that oxidative stress is involved in HepG2 cell senescence and growth inhibition, since different antioxidants partially and/or totally prevented SA- β -gal activity and cell viability loss.

Many anti-cancer drugs, including phytochemicals, target mitochondria and promote mitochondrial ROS generation, which in turn exacerbates mitochondrial dysfunction leading to mitochondrial membrane depolarization ($\Delta\Psi_m$ loss) [48]. There is increasing evidence that $\Delta\Psi_m$ loss may be an early trigger of cellular senescence through ROS production, ATP depletion, and AMPK activation [31,49]. In this study, 1,8-cineole induced moderate $\Delta\Psi_m$ loss at 8 mM after 3-h treatments, which paralleled the increase in ROS observed under the same conditions, suggesting a direct relationship between ROS production and $\Delta\Psi_m$ loss.

MAPKs, which include ERK, p38, and JNK kinases, are activated in response to stimuli such as mitogens or cellular stressors, including ROS [46]. While JNK activation is commonly associated with apoptosis induction, p38 and ERK have different roles, inducing cell proliferation, autophagic/senescent cell survival or cell death, depending on the cell type, intensity, and duration of the activation stimuli [11,12,14,32,41,46]. Indeed, ERK and p38 chronic signaling provoked by oxidative stress is one characteristic feature in senescent cancer cells [12,29,41].

Some studies state that 1,8-cineole modulates MAPK expression [19,21]. Here, we observed robust and sustained activation of both ERK and p38 at higher concentrations of 1,8-cineole, but no substantial changes in JNK. These and previous results together support the senescent phenotype observed and the absence of apoptotic features in 1,8-cineole-treated HepG2 cells.

AMPK (AMP-activated protein kinase) is an energy sensor protein that promotes the suppression of cell growth in response to low ATP levels, partially by inhibiting the mTORC1 pathway. Under stress conditions that cause ATP depletion (e.g., oxidative stress or $\Delta\Psi_m$ loss), AMPK may stimulate pro-survival autophagy, promote irreversible cell growth arrest or induce autophagic cell death [50–52]. Robust evidence suggests that oxidative stress-induced AMPK promotes cytoprotective autophagy before the senescent phenotype is established [51,53]. Some phytochemicals have been found to activate AMPK in HCC cells leading to autophagy and senescence [54,55]. Here, 1,8-cineole strongly elicited AMPK phosphorylation after 3 h, in correlation with a sharp decrease in p70S6K, augmented ROS production and $\Delta\Psi_m$ loss. These results suggest that 1,8-cineole-induced AMPK activation could be ROS- and $\Delta\Psi_m$ loss-dependent and that, even though no autophagic markers were evaluated here, AMPK-dependent mTOR inhibition could promote cytostatic autophagy as an early survival mechanism in response to a mild cellular insult [42].

Akt is a protein kinase that plays a central role in cell survival by inducing cell cycle protein synthesis through the activation of the mTORC1/p70S6K axis, diminishing p27 expression and suppressing pro-apoptotic proteins [56,57]. Akt signaling can be inhibited or activated by AMPK, depending on different factors, but the resulting phenotype is cell- and context-dependent [58]. Akt is induced by ROS, promoting pro-survival functions [59]. Our results showed that 1,8-cineole inhibited Akt phosphorylation at low concentrations, while higher amounts induced Akt phosphorylation, as we observed previously in the case of another monoterpene [25]. Choudhury et al. showed that AMPK activation with 5-aminoimidazole-4-carboxamide riboside (AICAR) activated or inhibited Akt signaling depending on the duration and intensity of the stimulus, but in both cases, mTOR signaling and tumor growth were inhibited, regardless of Akt status [60].

In our conditions, Akt phosphorylation increased from 1-h of treatment and peaked at 3 h at 1,8-cineole 8 mM; however, p70S6K remained highly inhibited, even after 24 h, suggesting that mTOR inhibition was strongly dependent on AMPK activation.

Inducing senescence in cancer cells appears to be a potent tool against cancer, including HCC [29,30,40]. Senescence-triggering anti-cancer drugs are effective not only because they robustly stop cancer cell growth but also because they promote a strong antitumor immune response [28–30,61]. While apoptosis is a cell-intrinsic response, senescent cells would have the advantage of communicating with neighboring cells and promoting their SASP phenotype, encouraging the immune system to clear both premalignant and established tumor cells [62]. Current evidence indicates that eliminating senescent tumor cells avoids the possible induction of cancer evolution favored by these cells via the SASP [29,30].

In this context, two families of anti-senescence drugs made their way into basic and medical research. While “senocidals” specifically eliminate senescent cells through apoptotic or non-apoptotic mechanisms, “senomorphics” suppress markers of the SASP [26,29,30,61]. Considering this, therapies with 1,8-cineole and senocidal/senomorphics drugs, combined or in tandem, could be a good strategy to potentiate the anti-cancer activity of each individual agent and avoid possible undesirable effects of senescence in cancer cells. We therefore evaluated combined and in tandem treatments of 1,8-cineole with four anti-senescence molecules, Qc, Sv, U, and SB, which selectively block the SASP and/or provoke senescent cell death [26–29]. Our results showed that 1,8-cineole and each compound strongly exacerbated cell growth inhibition in both combined and tandem treatments.

Statins are the lipid-lowering drugs that are most prescribed worldwide, but their antitumor efficacy has also been widely reported with both pre-clinical and clinical data, especially in combined therapies against cancer, including HCC [63]. We therefore assessed whether combined suboptimal concentrations of Sv and 1,8-cineole promoted HepG2 apoptosis, as a potential anti-cancer strategy capable of not only reducing the effective concentrations of each compound but also of evading the latent “dark side” of 1,8-cineole-induced senescence. As revealed here, the combined treatment effectively triggered apoptosis in HepG2 cells. Based on our findings, we propose a model for the mechanisms of action involved in HepG2 cell senescence induced by 1,8-cineole (Fig. 9).

5. Conclusions

Our study shows that 1,8-cineole promoted cell cycle arrest and ROS-induced senescence but not apoptosis in hepatocellular carcinoma HepG2 cells by regulating stress-activated AMPK, Akt/mTOR, and MAPK pathways. In addition, 1,8-cineole is capable of sensitizing HepG2 cells to anti-senescence drugs. These findings suggest that 1,8-cineole has a potential anti-cancer effect as a neoadjuvant or co-adjuvant molecule in combined therapies with antineoplastic drugs with senocidal and/or senomorphics properties.

Supplementary data to this article can be found online at <https://doi.org/10.1016/j.lfs.2020.117271>.

Declaration of competing interest

The authors declare that there are no conflicts of interest.

Acknowledgments

This work was supported by research grants from the Consejo Nacional de Investigaciones Científicas y Técnicas (CONICET), Agencia Nacional de Promoción Científica y Tecnológica (ANPCyT), and the Universidad Nacional de La Plata (UNLP), Argentina. Dr. B. Rodenak-Kladniew wants to thank the “Subsidio de Viajes UNLP 2016”, “Beca CONICET de Financiamiento Parcial para Estadías Posdoctorales en el

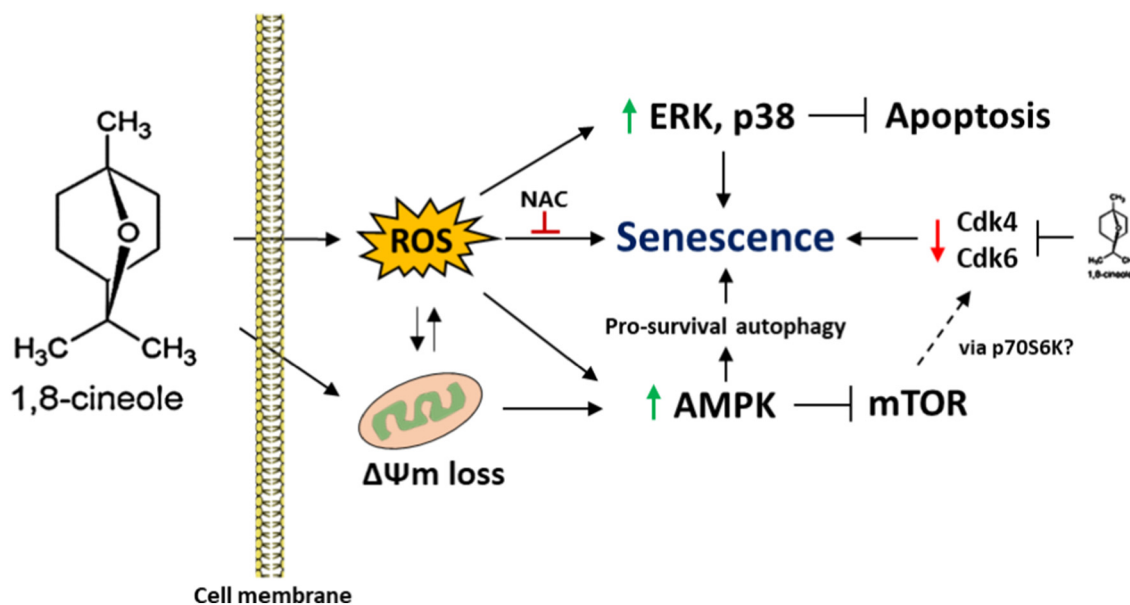


Fig. 9. A schematic drawing of the proposed mechanisms of 1,8-cineole-induced senescence in HepG2 cells. 1,8-Cineole induces ROS production and $\Delta\Psi_m$ depolarization, which promote ERK, p38 and AMPK activation, mTOR inhibition and decreased levels of Cdk 4 and 6, leading to G0/G1 cell cycle arrest and stress-induced senescence.

Exterior” and the “Programa de Retención de Doctores de la UNLP”. The authors are grateful to Dr. N. Scaglia, Dr. R. Goya and Mrs. R. del Cid from INIBIOLP for their collaboration in this work. We thank Joss Heywood, native speaker, for English language editing.

References

- [1] D.L. White, F. Kanwal, L. Jiao, H.B. El-Serag, Epidemiology of hepatocellular carcinoma, *Hepatocell. Carcinoma*, Springer, 2016, pp. 3–24.
- [2] J. Ferlay, I. Soerjomataram, R. Dikshit, S. Eser, C. Mathers, M. Rebelo, D.M. Parkin, D. Forman, F. Bray, Cancer incidence and mortality worldwide: sources, methods and major patterns in GLOBOCAN 2012, *Int. J. Cancer* 136 (2015).
- [3] J. Khazir, B.A. Mir, L.A. Pilcher, D.L. Riley, D.A. Cowan, *Anticancer Agents From Diverse Natural Sources*, (2014).
- [4] J. Fernandes, Antitumor monoterpenes, *Bioact. Essent. Oils Cancer*, Springer, 2015, pp. 175–200.
- [5] C. Wang, A. Cigliano, S. Delogu, J. Armbruster, F. Dombrowski, M. Evert, X. Chen, D. Calvisi, Functional crosstalk between AKT/mTOR and Ras/MAPK pathways in hepatocarcinogenesis: implications for the treatment of human liver cancer, *Cell Cycle* 12 (2013) 1999–2010.
- [6] S. Catalani, F. Palma, S. Battistelli, S. Benedetti, Oxidative stress and apoptosis induction in human thyroid carcinoma cells exposed to the essential oil from *Pistacia lentiscus* aerial parts, *PLoS One* 12 (2017) e0172138.
- [7] K. Nakayama, S. Murata, H. Ito, K. Iwasaki, M.O. Villareal, Y. Zheng, H. Matsui, H. Isoda, N. Ohkohchi, Terpinen-4-ol inhibits colorectal cancer growth via reactive oxygen species, *Oncol. Lett.* 14 (2017) 2015–2024.
- [8] C. Gorrini, I.S. Harris, T.W. Mak, Modulation of oxidative stress as an anticancer strategy, *Nat. Rev. Drug Discov.* 12 (2013) 931.
- [9] P. Storz, Reactive oxygen species in tumor progression, *Front. Biosci.* 10 (2005) 1881–1896.
- [10] S. Cagnol, J. Chambard, ERK and cell death: mechanisms of ERK-induced cell death—apoptosis, autophagy and senescence, *FEBS J.* 277 (2010) 2–21.
- [11] E. Panieri, V. Gogvadze, E. Norberg, R. Venkatesh, S. Orrenius, B. Zhivotovskiy, Reactive oxygen species generated in different compartments induce cell death, survival, or senescence, *Free Radic. Biol. Med.* 57 (2013) 176–187.
- [12] L. Tong, C.-C. Chuang, S. Wu, L. Zuo, Reactive oxygen species in redox cancer therapy, *Cancer Lett.* 367 (2015) 18–25.
- [13] J.A. Duke, S.M. Beckstrom-Sternberg, Dr. Duke’s Phytochemical and Ethnobotanical Databases, (1994).
- [14] F.A. Santos, V.S.N. Rao, Antiinflammatory and antinociceptive effects of 1, 8-cineole a terpenoid oxide present in many plant essential oils, *Phyther. Res. Int. J. Devoted Pharmacol. Toxicol. Eval. Nat. Prod. Deriv.* 14 (2000) 240–244.
- [15] A.C. Williams, B.W. Barry, Penetration enhancers, *Adv. Drug Deliv. Rev.* 64 (2012) 128–137.
- [16] G.R. Vilela, G.S. de Almeida, M.A.B.R. D’Arce, M.H.D. Moraes, J.O. Brito, M.F. das G.F. da Silva, S.C. Silva, S.M. de Stefano Piedade, M.A. Calori-Domingues, E.M. da Gloria, Activity of essential oil and its major compound, 1, 8-cineole, from *Eucalyptus globulus* Labill., against the storage fungi *Aspergillus flavus* Link and *Aspergillus parasiticus* Speare, *J. Stored Prod. Res.* 45 (2009) 108–111.
- [17] S. Murata, R. Shiragami, C. Kosugi, T. Tezuka, M. Yamazaki, A. Hirano, Y. Yoshimura, M. Suzuki, K. Shuto, N. Ohkohchi, Antitumor effect of 1, 8-cineole against colon cancer, *Oncol. Rep.* 30 (2013) 2647–2652.
- [18] H. Moteki, H. Hibasami, Y. Yamada, H. Katsuzaki, K. Imai, T. Komiya, Specific induction of apoptosis by 1, 8-cineole in two human leukemia cell lines, but not in a human stomach cancer cell line, *Oncol. Rep.* 9 (2002) 757–760.
- [19] J.-D. Cha, Y.-H. Kim, J.-Y. Kim, Essential oil and 1, 8-cineole from *Artemisia lavalandulaefolia* induces apoptosis in KB cells via mitochondrial stress and caspase activation, *Food Sci. Biotechnol.* 19 (2010) 185–191.
- [20] S. Sampath, S. Subramani, S. Janardhanam, P. Subramani, A. Yuvaraj, R. Chellan, Bioactive compound 1, 8-cineole selectively induces G2/M arrest in A431 cells through the upregulation of the p53 signaling pathway and molecular docking studies, *Phytomedicine* 46 (2018) 57–68.
- [21] B. Rodenak Kladniew, M. Polo, S. Montero Villegas, M. Galle, R. Crespo, M. García De Bravo, Synergistic antiproliferative and anticholesterogenic effects of linalool, 1,8-cineole, and simvastatin on human cell lines, *Chem. Biol. Interact.* 214 (2014) 57–68.
- [22] G.P. Dimri, X. Lee, G. Basile, M. Acosta, G. Scott, C. Roskelley, E.E. Medrano, M. Linskens, I. Rubelj, O. Pereira-Smith, A biomarker that identifies senescent human cells in culture and in aging skin in vivo, *Proc. Natl. Acad. Sci.* 92 (1995) 9363–9367.
- [23] B. Rodenak-Kladniew, A. Castro, P. Stärkel, C. De Saeger, M.G. de Bravo, R. Crespo, Linalool induces cell cycle arrest and apoptosis in HepG2 cells through oxidative stress generation and modulation of Ras/MAPK and Akt/mTOR pathways, *Life Sci.* 199 (2018) 48–59.
- [24] J.L. Kirkland, T. Tchkonja, Y. Zhu, L.J. Niedernhofer, P.D. Robbins, The clinical potential of senolytic drugs, *J. Am. Geriatr. Soc.* 65 (2017) 2297–2301.
- [25] S. Liu, H. Uppal, M. Demaria, P.-Y. Desprez, J. Campisi, P. Kapahi, Simvastatin suppresses breast cancer cell proliferation induced by senescent cells, *Sci. Rep.* 5 (2015) 17895.
- [26] A. Soto-Gamez, M. Demaria, Therapeutic interventions for aging: the case of cellular senescence, *Drug Discov. Today* 22 (2017) 786–795.
- [27] V. Myrianthopoulos, K. Evangelou, P.V.S. Vasileiou, T. Cooks, T.P. Vassilakopoulos, G.A. Pangalis, M. Kouloukoussa, C. Kittas, A.G. Georgakilas, V.G. Gorgoulis, Senescence and senotherapeutics: a new field in cancer therapy, *Pharmacol. Ther.* 193 (2018) 31–49.
- [28] A. Calcinotto, A. Alimonti, Aging tumour cells to cure cancer: “pro-senescence” therapy for cancer, *Swiss Med. Wkly.* 147 (2017).
- [29] D.V. Ziegler, C.D. Wiley, M.C. Velarde, Mitochondrial effectors of cellular senescence: beyond the free radical theory of aging, *Aging Cell* 14 (2015) 1–7.
- [30] E.F. Wagner, Á. Nebreda, Signal integration by JNK and p38 MAPK pathways in cancer development, *Nat. Rev. Cancer* 9 (2009) 537.
- [31] B. Dörsam, C.-F. Wu, T. Efferth, B. Kaina, J. Fahrner, The eucalyptus oil ingredient 1, 8-cineole induces oxidative DNA damage, *Arch. Toxicol.* 89 (2015) 797–805.
- [32] T. Efferth, F. Herrmann, A. Tahrani, M. Wink, Cytotoxic activity of secondary metabolites derived from *Artemisia annua* L. towards cancer cells in comparison to its designated active constituent artemisinin, *Phytomedicine* 18 (2011) 959–969.
- [33] W. Wang, N. Li, M. Luo, Y. Zu, T. Efferth, Antibacterial activity and anticancer activity of *Rosmarinus officinalis* L. essential oil compared to that of its main components, *Molecules* 17 (2012) 2704–2713.
- [34] J. Nair, P. Muley, S. Dutt, Therapy induced senescence and its implications in cancer, *Cancer* 1 (2017) 1–2.
- [35] I. Fabregat, Dysregulation of apoptosis in hepatocellular carcinoma cells, *World J.*

- Gastroenterol. 15 (2009) 513.
- [38] P.B.S. Lai, T.-Y. Chi, G.G. Chen, Different levels of p53 induced either apoptosis or cell cycle arrest in a doxycycline-regulated hepatocellular carcinoma cell line in vitro, *Apoptosis* 12 (2007) 387–393.
- [39] O.V. Leontieva, M.V. Blagosklonny, CDK4/6-inhibiting drug substitutes for p21 and p16 in senescence: duration of cell cycle arrest and MTOR activity determine geronconversion, *Cell Cycle* 12 (2013) 3063–3069.
- [40] M. Ozturk, A. Arslan-Ergul, S. Bagislar, S. Senturk, H. Yuzugullu, Senescence and immortality in hepatocellular carcinoma, *Cancer Lett.* 286 (2009) 103–113.
- [41] A. Borodkina, A. Shatrova, P. Abushik, N. Nikolsky, E. Burova, Interaction between ROS dependent DNA damage, mitochondria and p38 MAPK underlies senescence of human adult stem cells, *Aging (Albany NY)* 6 (2014) 481.
- [42] A. Lewinska, J. Adamczyk-Grochala, E. Kwasniewicz, A. Deregowska, M. Wnuk, Diosmin-induced senescence, apoptosis and autophagy in breast cancer cells of different p53 status and ERK activity, *Toxicol. Lett.* 265 (2017) 117–130.
- [43] R.L. de Oliveira, R. Bernards, Anti-cancer therapy: senescence is the new black, *EMBO J.* 37 (2018) e99386.
- [44] U.-M. Chang, C.-H. Li, L.-I. Lin, C.-P. Huang, L.-S. Kan, S.-B. Lin, Ganoderiol F, a ganoderma triterpene, induces senescence in hepatoma HepG2 cells, *Life Sci.* 79 (2006) 1129–1139.
- [45] F.-H. Gao, X.-H. Hu, W. Li, H. Liu, Y.-J. Zhang, Z.-Y. Guo, M.-H. Xu, S.-T. Wang, B. Jiang, F. Liu, Oridonin induces apoptosis and senescence in colorectal cancer cells by increasing histone hyperacetylation and regulation of p16, p21, p27 and c-myc, *BMC Cancer* 10 (2010) 610.
- [46] G.-Y. Liou, P. Storz, Reactive oxygen species in cancer, *Free Radic. Res.* 44 (2010) 479–496.
- [47] A. Aravinthan, N. Shannon, J. Heaney, M. Hoare, A. Marshall, G.J.M. Alexander, The senescent hepatocyte gene signature in chronic liver disease, *Exp. Gerontol.* 60 (2014) 37–45.
- [48] S. Fulda, L. Galluzzi, G. Kroemer, Targeting mitochondria for cancer therapy, *Nat. Rev. Drug Discov.* 9 (2010) 447.
- [49] O. Moiseeva, V. Bourdeau, A. Roux, X. Deschênes-Simard, G. Ferbeyre, Mitochondrial dysfunction contributes to oncogene-induced senescence, *Mol. Cell. Biol.* 29 (2009) 4495–4507.
- [50] X. Jiang, H.-Y. Tan, S. Teng, Y.-T. Chan, D. Wang, N. Wang, The role of AMP-activated protein kinase as a potential target of treatment of hepatocellular carcinoma, *Cancers* 11 (2019) 647.
- [51] X. Han, H. Tai, X. Wang, Z. Wang, J. Zhou, X. Wei, Y. Ding, H. Gong, C. Mo, J. Zhang, AMPK activation protects cells from oxidative stress-induced senescence via autophagic flux restoration and intracellular NAD⁺ elevation, *Aging Cell* 15 (2016) 416–427.
- [52] M.M. Mihaylova, R.J. Shaw, The AMPK signalling pathway coordinates cell growth, autophagy and metabolism, *Nat. Cell Biol.* 13 (2011) 1016.
- [53] Y. Wang, Y. Liang, P.M. Vanhoutte, SIRT1 and AMPK in regulating mammalian senescence: a critical review and a working model, *FEBS Lett.* 585 (2011) 986–994.
- [54] I.-J. Park, W.K. Yang, S.-H. Nam, J. Hong, K.R. Yang, J. Kim, S.S. Kim, W. Choe, I. Kang, J. Ha, Cryptotanshinone induces G1 cell cycle arrest and autophagic cell death by activating the AMP-activated protein kinase signal pathway in HepG2 hepatoma, *Apoptosis* 19 (2014) 615–628.
- [55] X. Li, Y. Wang, Y. Xiong, J. Wu, H. Ding, X. Chen, L. Lan, H. Zhang, Galangin induces autophagy via deacetylation of LC3 by SIRT1 in HepG2 cells, *Sci. Rep.* 6 (2016) 30496.
- [56] D.C. Fingar, C.J. Richardson, A.R. Tee, L. Cheatham, C. Tsou, J. Blenis, mTOR controls cell cycle progression through its cell growth effectors S6K1 and 4E-BP1/eukaryotic translation initiation factor 4E, *Mol. Cell. Biol.* 24 (2004) 200–216.
- [57] F. Chang, J.T. Lee, P.M. Navolanic, L.S. Steelman, J.G. Shelton, W.L. Blalock, R.A. Franklin, J.A. McCubrey, Involvement of PI3K/Akt pathway in cell cycle progression, apoptosis, and neoplastic transformation: a target for cancer chemotherapy, *Leukemia* 17 (2003) 590.
- [58] W. Li, S.M. Saud, M.R. Young, G. Chen, B. Hua, Targeting AMPK for cancer prevention and treatment, *Oncotarget.* 6 (2015) 7365.
- [59] N. Hay, The Akt-mTOR tango and its relevance to cancer, *Cancer Cell* 8 (2005) 179–183.
- [60] Y. Choudhury, Z. Yang, I. Ahmad, C. Nixon, I.P. Salt, H.Y. Leung, AMP-activated protein kinase (AMPK) as a potential therapeutic target independent of PI3K/Akt signaling in prostate cancer, *Oncoscience* 1 (2014) 446.
- [61] B.G. Childs, M. Gluscevic, D.J. Baker, R.-M. Laberge, D. Marquess, J. Dananberg, J.M. van Deursen, Senescent cells: an emerging target for diseases of ageing, *Nat. Rev. Drug Discov.* 16 (2017) 718.
- [62] B.G. Childs, D.J. Baker, J.L. Kirkland, J. Campisi, J.M. van Deursen, Senescence and apoptosis: dueling or complementary cell fates? *EMBO Rep.* 15 (2014) 1139–1153.
- [63] M. Osmak, Statins and cancer: current and future prospects, *Cancer Lett.* 324 (2012) 1–12.